

Mannose-Modified Liposome Co-Delivery of Human Papillomavirus Type 16 E7 Peptide and CpG Oligodeoxynucleotide Adjuvant Enhances Antitumor Activity Against Established Large TC-1 Grafted Tumors in Mice

This article was published in the following Dove Press journal:
International Journal of Nanomedicine

Yan Zhao¹
Huan Wang²
Yang Yang²
Wendan Jia¹
Tong Su¹
Yuxin Che²
Yixin Feng¹
Xuemei Yuan¹
Xuelian Wang²

¹Department of Pharmaceutics, School of Pharmacy, China Medical University, Shenyang 110122, People's Republic of China; ²Department of Microbiology and Parasitology, College of Basic Medical Sciences, China Medical University, Shenyang 110122, People's Republic of China

Background: Previously, we demonstrated the therapeutic efficacy of a human papillomavirus (HPV) vaccine, including HPV16 E7 peptide and CpG oligodeoxynucleotides (CpG ODN), against small TC-1 grafted tumors. Here, we developed an HPV16 E7 peptide and CpG ODN vaccine delivered using liposomes modified with DC-targeting mannose, Lip E7/CpG, and determined its anti-tumor effects and influence on systemic immune responses and the tumor microenvironment (TME) in a mouse large TC-1 grafted tumor model.

Methods: L-alpha-phosphatidyl choline (SPC), cholesterol (CHOL), 1,2-distearoyl-*sn*-glycero-3-phosphoethanolamine-N-[methoxy (polyethylene glycol-2000)] (DSPE-PEG-2000), 1,2-dioleoyl-3-trimethylammonium-propane chloride salt (DOTAP) and Mannose-PEG-DSPE, loaded with HPV16 E7 peptide and CpG ODN, were used to construct the Lip E7/CpG vaccine. The anti-tumor effects and potential mechanism of Lip E7/CpG were assessed by assays of tumor growth inhibition, immune cells, in vivo cytotoxic T lymphocyte (CTL) responses and cytokines, chemokines, CD31, Ki67 and p53 expression in the TME. In addition, toxicity of Lip E7/CpG to major organs was evaluated.

Results: Lip E7/CpG had a diameter of 122.21 ± 8.37 nm and remained stable at 4°C for 7 days. Co-delivery of HPV16 E7 peptide and CpG ODN by liposomes exerted potent anti-tumor effects in large (tumor volume $\geq 200\text{mm}^3$) TC-1 grafted tumor-bearing mice with inhibition rates of 80% and 78% relative to the control and Free E7/CpG groups, respectively. Vaccination significantly increased numbers of CD4+ and CD8+ T cells, and IFN- γ -producing cells in spleens and tumors and enhanced HPV-specific CTL responses, while reducing numbers of inhibitory cells including myeloid-derived suppressor cells and macrophages. Expression of cytokines and chemokines was altered and formation of tumor blood vessels was reduced in the Lip E7/CpG group, indicating possible modulation of the immunosuppressive TME to promote anti-tumor responses. Lip E7/CpG did not cause morphological changes in major organs.

Conclusion: Lip E7/CpG induced anti-tumor effects by enhancing cellular immunity and improving tumor-associated immunosuppression. Mannose-modified liposomes are the promising vaccine delivery strategy for cancer immunotherapy.

Keywords: immunotherapy, human papillomavirus, peptide vaccine, CpG ODN adjuvant, liposome, tumor microenvironment

Correspondence: Xuelian Wang
Email xlwang18@cmu.edu.cn

Introduction

Treatment of cancer remains a challenge worldwide. Detection of tumors at primary stages and prompt commencement of surgical treatment combined with chemotherapy and radiotherapy is an effective treatment strategy with the best prognosis.¹ When patients present with locally advanced, metastatic, or recurrent stage disease, when the potential for conventional anti-tumor therapy is limited, immunotherapy can be used as a novel strategy to improve outcomes. Immunotherapy approaches, including peptide vaccination, adoptive T-cell therapy, and immune checkpoint inhibition, have shown promising objective response rates and led to improved survival in patients who fail to respond to standard therapies.²⁻⁴

As one of the most developed immunotherapy approaches, peptide vaccines have achieved tremendous scientific advances because of their unique advantages. Peptide vaccines constituting highly purified peptides are at the forefront of vaccine research, owing to their strong safety profile, relative ease of production, and low production costs, relative to classical live attenuated or killed vaccines; however, peptide vaccines generally show poor immunogenicity due to rapid degradation *in vivo*, which reduces their dose-effectiveness.^{5,6}

In our previous study, we investigated the anti-tumor effect of an HPV peptide vaccine, including CpG oligodeoxynucleotides (CpG ODN) 1826 as an adjuvant and HPV16 E7 43–77 peptide as an antigen, which contains a CD8 T cell epitope (E7 49–57), and two CD4 T cell epitopes (E7 43–77 and E7 50–62). A single administration of the vaccine before and 4 days after inoculation with TC-1 cells expressing HPV16 E6/E7 induced immune responses and resulted in significant prophylactic and therapeutic effects on TC-1 grafted tumors in mice;⁷ however, this approach was less successful when used at later stages of tumor growth. Evidence indicated that the surviving tumor cells developed various mechanisms to avoid immune recognition and elimination during tumor progression, offsetting the effects of a theoretically efficient immunotherapy.^{8,9} Therefore, development of an effective immunotherapy against locally advanced cancers remains a challenge.

Antigen presenting cells, especially dendritic cells (DCs), are important in peptide vaccine processing to induce an effective immune response *in vivo*.¹⁰ After DCs phagocytose peptide vaccine, they migrate to the

lymph nodes and present antigens on their surface via major histocompatibility complex class I (MHC-I) and II (MHC-II) molecules, thereby stimulating the differentiation of naïve CD8+ T cells into cytotoxic T lymphocytes (CTLs), and CD4+ T cells into a variety of T cell subsets, respectively.¹¹ Optimal antigen loading and activation of DCs is crucial for initiation of an efficient immune response. The identification of DC-specific receptors has promoted the development of DC-targeting vaccines. DCs express mannose receptors (belonging to the C-type lectin receptor family) and DC-specific receptors (such as CD205 and DC-SIGN),^{12,13} targeting and activation of which can enhance DC-mediated antitumor activities. Further, delivery of tumor-specific antigen alongside appropriate DC maturation stimuli is critical for improving immunotherapeutic effects.^{14,15} CpG ODN acts as a potent adjuvant for activation of immature DCs via Toll-like receptor 9 (TLR9) and plays essential roles in both immune response initiation and breaking pre-existing immune tolerance.¹⁶

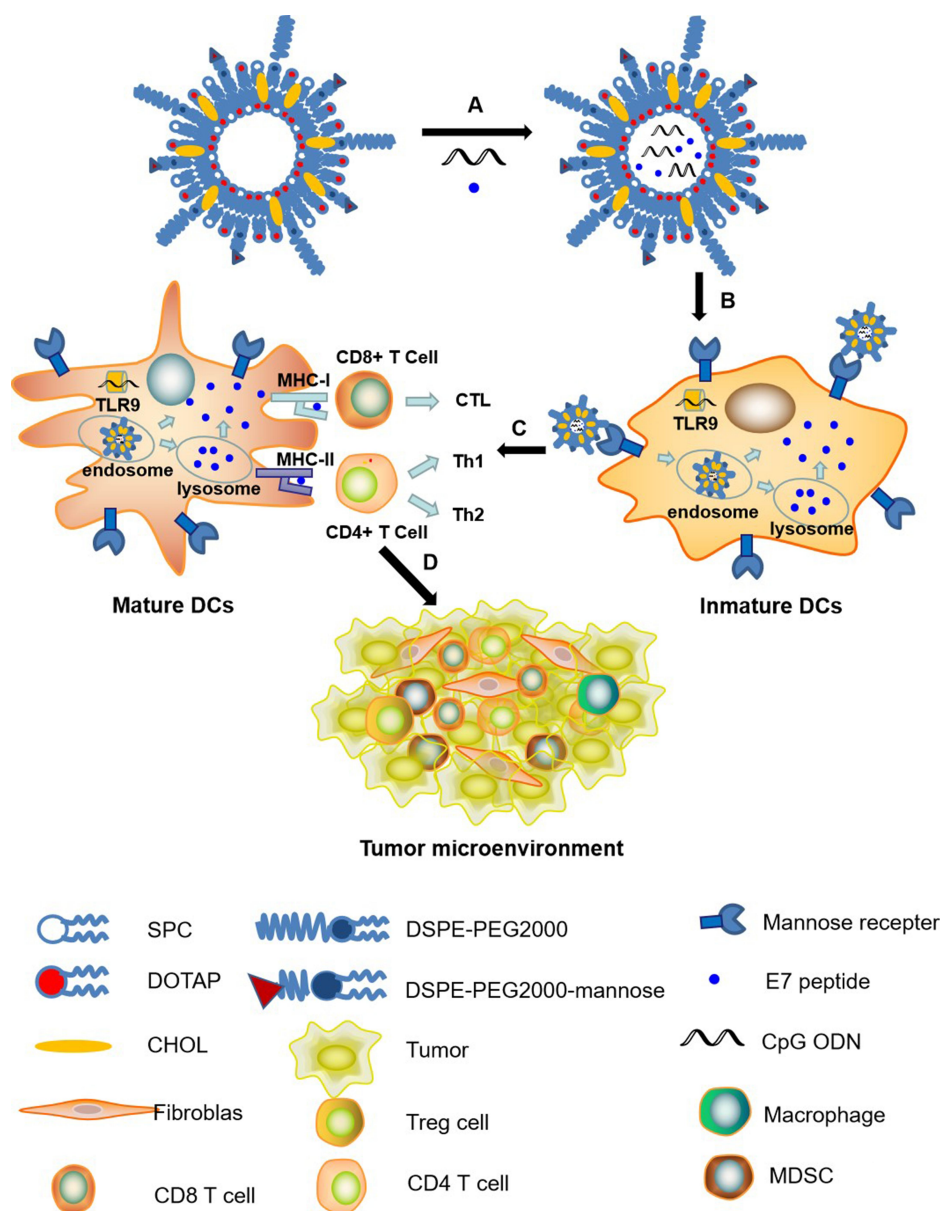
Liposomes and liposome-derived nanovesicles, which elicit both antigen-specific cell-mediated and humoral immunity, are considered excellent vaccine delivery carriers/adjuvants.¹⁷ Owing to their self-enclosed structures, liposomes can entrap hydrophobic agents within the lipid bilayer and hydrophilic agents in their aqueous compartment.¹⁸ Further, they protected the loaded drug, avoiding both degradation and undesirable effects of exposure to the environment on drug activity. Mannose-modified liposomes can not only co-deliver peptides and CpG ODN, but also specifically target mannose receptors on DCs, thus enhancing DC-mediated antitumor activity.^{19,20}

In this study, to efficiently target and activate DCs, mannose-modified liposomes encapsulating HPV16 E7 peptide and CpG ODN were constructed and the therapeutic efficacy of this vaccine on large (volume over than 200 mm³) TC-1 grafted tumors was evaluated. *In vivo* studies were performed to investigate the mechanisms involved in the anti-tumor responses induced by the vaccine formulation. **Scheme 1** provided a mechanism for the construction of peptide vaccine and the putative anti-tumor effects.

Materials and Methods

Materials

L-alpha-phosphatidyl choline (SPC), cholesterol (CHOL), 1,2-distearoyl-*sn*-glycero-3-phosphoethanolamine-N-[methoxy (polyethylene glycol-2000)] (DSPE-PEG-2000), and



Scheme 1 Schematic description of the preparation and function of Lip E7/CpG. (A) Encapsulation of E7 peptide and CpG ODN adjuvant in Lip E7/CpG; (B) binding of mannose with mannose receptors on DCs surfaces; (C) after entry into DCs, Lip E7/CpG is delivered to the endosomes, enabling the activation and maturation of DCs, simultaneously, inducing CD4+ T cells and CD8+ T cells immune responses; (D) activated CD4+ T cells and CD8+ T cells migrated into the tumor microenvironment to kill tumor cells.

1,2-distearoyl-*sn*-glycero-3-phosphoethanolamine-*N*-[succinimidyl (polyethylene glycol)-2000] (DSPE-PEG-NHS) were purchased from Shanghai Toshisun Biology & Technology Co. Ltd. (Shanghai, China). 1,2-dioleoyl-3-trimethylammonium-propane chloride salt (DOTAP) was purchased from Shanghai Advanced Vehicle Technology Pharmaceutical Ltd. (Shanghai, China) and 4-Amino phenyl α -D-mannopyranoside was from Aladdin (Shanghai, China). Mannose-PEG-DSPE was synthesized using DSPE-PEG-

NHS and 4-Amino phenyl α -D-mannopyranoside, as previously reported, and the structure confirmed using $^1\text{H-NMR}$.

HPV16 E7 43–77 (GQAEPDRAHYNIVTFCKCDST LRLCVQSTHVDIR) and OVA 257–264 (SIINFEKL) peptides were synthesized by GL Biochem Ltd (Shanghai, China). Peptide purity was determined to be >95% by high-pressure liquid chromatography (HPLC) and peptide sequences were validated by mass spectrometry (MALDI-TOF). CpG ODN 1826 (5'-TCCATG

ACGTCCTGACGTT-3') was synthesized by Sangon Biotech Co. Ltd. (Shanghai, China).

FITC-conjugated anti-mouse CD4, PerCP-conjugated anti-mouse CD8a, FITC-conjugated anti-mouse Gr-1, PerCP-conjugated anti-mouse CD11b, PE-conjugated anti-mouse F4/80, PE-conjugated anti-mouse IFN- γ , and PE-conjugated anti-mouse FoxP3 were purchased from Biolegend (San Diego, CA, USA). Ionomycin and Phorbol 12-myristate 13-acetate were from Sigma-Aldrich (Louis, MO, USA). Golgiplug was obtained from BD Biosciences (San Diego, CA, USA).

Cell Lines and Mice

The murine tumor cell line TC-1 (HPV-16 E6/E7 and c-Ha-Ras co-transformed mouse lung epithelial cells) was obtained from the Beijing Beina Chuanglian Biotechnology Institute (Beijing, China). TC-1 cells were cultured in Roswell Park Memorial Institute 1640 medium supplemented with 10% fetal calf serum, 2 mM G418, 100 U/mL penicillin, and 100 μ g/mL streptomycin at 37°C under 10% carbon dioxide.⁷

Female *C57BL/6* mice (6–8 weeks old) were purchased from Liaoning Changsheng Biotechnology Co. Ltd (Benxi, China). Animal care and use were performed according to a protocol reviewed and approved by the Institutional Animal Care and Use Committee (IACUC) of China Medical University (IACUC Issue No. CMU2019293).

Preparation and Characterization of the Liposome-Based Vaccine

A liposome vaccine for co-delivery of E7 peptide and CpG ODN was prepared using the reverse-phase evaporation method. Briefly, SPC, CHOL, DOTAP, DSPE-PEG-2000, and DSPE-PEG-2000-mannose were dissolved in chloroform, and then PBS containing E7 peptide and CpG ODN was injected into the chloroform solution. The mixture was homogenized using a probe ultrasound in an ice bath to form a stable water-in-oil type emulsion. Subsequently, the chloroform was evaporated from the emulsion to form a colloid by rotary vacuum evaporation, and then PBS solution was added to hydrate for 15 min. The resulting mixture was then homogenized again by probe ultrasonic treatment to form well-proportioned liposomes. Finally, the liposomes were filtered using 0.45 and 0.22 μ m Millipore membranes and purified by ultrafiltration (50,000 NMWL, Millipore) at 4000 g for 15 min to remove the unloaded E7 peptide and CpG ODN. The

liposome vaccine was then re-suspended and collected. To evaluate the stability of the liposome-based vaccine, the liposomal particles were stored at 4°C for up to 7 days.

E7 peptide was measured using HPLC (Waters e2695 and 2489, USA), and CpG ODN by agarose gel electrophoresis, respectively. Entrapment efficiency (EE) was calculated according to the formulas:

$$EE = \frac{\text{Amounts of drug in liposomes}}{\text{Total amount of drug}} \times 100\%$$

Morphology of the liposome-based vaccine was observed using transmission electron microscopy (TEM) (JEOL 100CX II, Japan). Particle size distributions and zeta potential were measured using a Laser Particle size analyzer in water (PSS NICOMP TM 380, USA).

Tumor Growth Inhibition

Female *C57BL/6* mice were inoculated subcutaneously in their flanks with 5×10^5 TC-1 cells on day 0. On day 12, formulations (control, empty liposome, free E7/CpG, and lip E7/CpG) were subcutaneously injected into the contralateral side from the tumor cell inoculation side. Thereafter, tumor size was measured using digital calipers every 2–3 days and tumor volume was calculated as: Tumor volume (mm^3) = $0.5 \times \text{length} \times \text{width}^2$. Body weight was also monitored.

Flow Cytometry Assay

On days 28, spleens and tumors were harvested. Single cell suspensions were prepared as described in our previous study.²¹ The dissociated cells were dispersed in PBS ($1 \times 10^6/\text{mL}$) and stained for surface, intracellular and intranuclear molecules. Analysis was performed on a FACS Calibur flow cytometer (Becton Dickinson, USA) using FlowJo X software (Treestar, Ashland, OR, USA).

Surface Molecule Staining

For analysis of surface molecules associated with CD4+ T cells, CD8+ T cells, regulatory T cells (Tregs), myeloid-derived suppressor cells (MDSCs), and macrophages, single cell suspensions from spleens and tumors were stained with the following fluorescein-conjugated antibodies: FITC-conjugated anti-mouse CD4, PerCP-conjugated anti-mouse CD8a, FITC-conjugated anti-mouse Gr-1, PerCP-conjugated anti-mouse CD11b and PE-conjugated anti-mouse F4/80 (all the above antibodies were from Biolegend, San Diego, CA, USA).

Intracellular Cytokine Staining

Splenocytes were incubated with peptide E7 (43–77) for 5 h, then with Golgiplug for 4 h. Single cell suspensions from tumors were incubated with the ionomycin (50 µg/mL, Sigma-Aldrich St. Louis, MO, USA) and phorbol 12-myristate 13-acetate (PMA, 1 µg/mL) (Sigma-Aldrich, St. Louis, MO, USA) for 5 h, then with Golgiplug (BD Biosciences, San Diego, CA, USA) for the final 4 h. Following stimulation, cells were stained with PE-conjugated anti-mouse IFN-γ (Biolegend, San Diego, CA, USA).

Intranuclear Transcription Factor Staining

For analysis of Tregs, intranuclear staining was conducted by adding PE-conjugated anti-mouse FoxP3 (Biolegend, San Diego, CA, USA), following fixation and membrane permeation.

Assessment of in vivo CTL Responses

In vivo CTL assays were performed according to a previously described protocol.²² In brief, splenocytes from naïve *C57BL/6* mice were collected and loaded with either 10 µM E7 or Ova peptides in complete media at 37°C for 1 h. Then, the E7-pulsed and Ova-pulsed cells were labeled with 4 and 0.4 µM CFSE, respectively. Seven days after vaccination, an equal amount of CFSE^{high} (E7-pulsed cells) and CFSE^{low} (Ova-pulsed cells) were mixed and injected into the tail veins of treated mice. Eighteen hours later, splenocytes were collected and subjected to flow cytometry analysis. The numbers of CFSE^{high} and CFSE^{low} were counted and the percentage of E7-specific in vivo lysis was calculated according to a published equation, as follows:

$$\% \text{ specific lysis} = \frac{(Ova \times x - E7)}{(Ova \times x)} \times 100\%$$

$$\text{where } x = \frac{E7}{Ova} \text{ from naive mice}$$

Quantitative Real-Time PCR Assay

Total RNA was extracted from tumor tissue samples using Trizol reagent (Invitrogen, Carlsbad, CA, USA) and 0.5 µg of total RNA was used as template for first-strand cDNA synthesis using a Reverse Transcription System (Promega, Madison, WI, USA), according to the manufacturer's protocols: reaction conditions, 50°C for 15 min and 85°C for 5 s. Amplification was conducted using SYBR qPCR Master Mix for RT-PCR (Vazyme, Nanjing, China), mouse-specific primers, and cDNA. RT-PCR conditions were as follows: 95°C for 30 s, 95°C for 10 s, and 60°C for 30 s, for 40 cycles. All mouse-specific primers (Shenggong, Shanghai, China) for RT-PCR were described in our previous study²¹ and are listed in Table 1. β-actin was used as an endogenous control. Reactions were conducted using a 7500 Real-Time PCR System, and data was analyzed with 7500 Software.

Immunohistochemistry

Fresh tumor tissues were removed and immersed in 4% paraformaldehyde for 48h, then embedded in paraffin blocks. Sections were deparaffinization and rehydrated, then incubated in 3% H₂O₂ at 37°C for 25 min. Slides were treated with citric acid buffer at 95°C for 10 min, and non-specific binding was blocked using goat serum at 37°C for 30 min, followed by incubation with primary antibodies against CD31, Ki67, and p53 at 4°C overnight, then biotinylated secondary antibody at 37°C for 30 min. Antibody complexes were detected by incubation with a streptavidin-biotin-horseradish peroxidase complex and color was developed using diaminobenzidine. Slides were counterstained with hematoxylin for 5 min,²³ and preparations examined under

Table 1 Primers for RT-PCR Reactions

Gene	Forward (5'-3')	Reverse (5'-3')
<i>β-actin</i>	CATCCGTAAAGACCTCTATGCCAAC	ATGGAGCCACCGATCCACA
<i>IFN-γ</i>	ACTCMGTGGCATAGATGTGGMG	GACGCTTATGTTGTTGCTGATGG
<i>TNF-α</i>	CCAACATGCTGATTGATGACACC	GAGAATGCCAATTTTGATTGCCA
<i>TGF-β1</i>	CTCCCACTCCCGTGGCTTCTAG	GTTCCACATGTTGCTCCACACTGG
<i>IL-2</i>	AAGCTCTACAGCGGAAGCAC	TCATCGAATTGGCACTCAA
<i>IL-4</i>	TAGTTGTCATCCTGCTCTT	GTCTTTCAGTGATGTGGAC
<i>IL-12</i>	CAATCACGCTACCTCCTCTTTT	CAGCAGTGCAGGAATAATGTTTC
<i>CCL-3</i>	TGAGAGTCTTGGAGGCAGC	ATGCAGGTGGCAGGAATG
<i>CXCL-9</i>	CTTGAGCCTAGTCGTGATAAC	CCAGCTTGGTGAGGTCTATC
<i>CXCL-10</i>	TCCTTGTCCTCCCTAGCTCA	ATAACCCCTTGGGAAGATGG

a light microscope (Nikon 80i, Japan). Ten randomly selected microscopic fields were used for quantitative analysis.

Hematoxylin-Eosin Staining

Tumor-bearing mice were treated and sacrificed at the designated time points. The major organs were quickly harvested and immersed in paraformaldehyde for 48 h. Fixed tissues were embedded in paraffin and 5 μm histological sections were prepared. Sections were stained with hematoxylin and eosin (HE) and then subjected to microscopic examination and photography.²² The morphological features of the tissue were observed to analyze tissue injury.

Statistical Analysis

Calculations were performed using GraphPad Prism version 5.0. Data are described as means \pm standard deviation (SD). Statistical significance was analyzed by one-way analysis of variance (ANOVA), followed by Tukey's multiple comparisons test. Differences were considered statistically significant if the *p* value was <0.05 .

Results

Characterization of the Liposome-Based Vaccine

Observation by TEM after negative staining showed that Lip E7/CpG had a spherical structure with diameter ranging from 60–120 nm (Figure 1A). Similarly, measurement by dynamic light scattering indicated a mean \pm SD diameter of 122.21 ± 8.37 nm (Figure 1B). Particle size, polydispersity index (PDI), zeta potential, and EE of Lip E7/CpG are listed in Table 2. Lip E7/CpG exhibited good stability within

7 days after storage at $4^\circ\text{C} \pm 2^\circ\text{C}$; specifically, particle size and EE showed little change within 7 days, indicating that they were consistent throughout the experiments.

Inhibition of Tumor Growth by Therapeutic Vaccine

All tested formulations were injected subcutaneously on day 12, mean tumor size was >200 mm³. Equal amounts of E7 peptide (50 μg) and CpG ODN (20 μg) were applied. As shown in Figure 2, neither empty liposome (designated “Empty Lip”) nor free E7 combined with CpG ODN (designated “Free E7/CpG”) had any therapeutic effect on large TC-1 grafted tumors, while DCs-targeting liposomes loaded with HPV16 E7 peptide and CpG ODN (designated “Lip E7/CpG”) achieved 80% and 78% tumor growth inhibition on day 28, relative to the Control and Free E7/CpG groups, respectively. There was no decrease in body weight in any group.

Lip E7/CpG Enhanced Systemic and Local Immune Responses

We determined the percentages of CD4+ T cells, CD8+ T cells and IFN- γ -producing cells in spleens and tumors. The percentage of CD4+ T cells, CD8+ T cells and IFN- γ -producing cells were significantly increased in the Lip E7/CPG group compared with the control, Empty Lip and Free E7/CPG groups (Figures 3 and 5).

To evaluate the systemic and tumor microenvironment (TME) immunosuppressive responses induced by the vaccine, we determined the percentages of Tregs, MDSCs and macrophages in the spleens and tumors. Splenocytes of

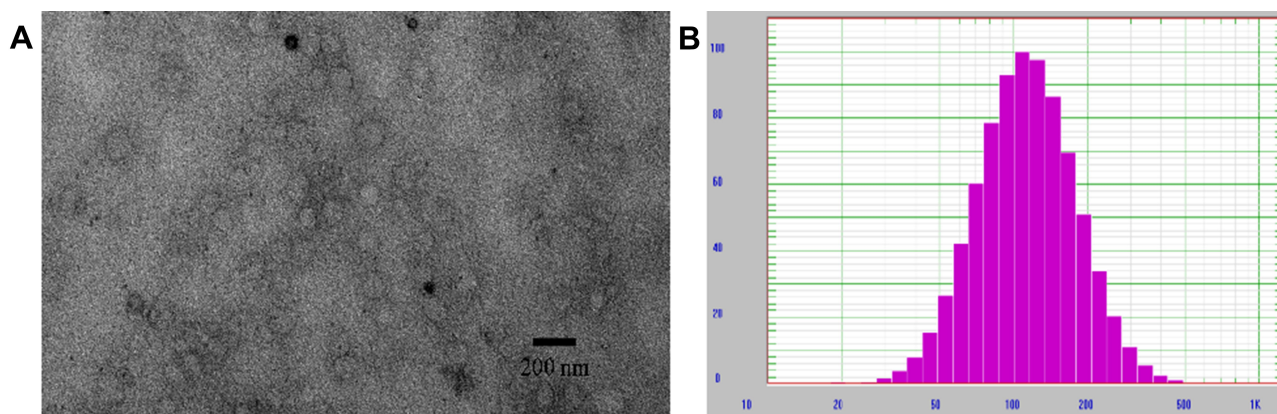


Figure 1 Physicochemical characterization of liposomes containing E7 peptide and CPG ODN adjuvant. (A) TEM images of liposomes after negative staining. (B) DLS size distribution of liposomes.

Table 2 Particle Size, PDI, Zeta Potential and EE of Lip E7/CpG After Storage at 4°C ± 2°C (n=3)

Time (d)	Particle Size (nm, ± SD)	PDI (± SD)	Zeta Potential (mV, ± SD)	EE of E7 Peptide (% , ± SD)	EE of CpG ODN (% , ± SD)
0	122.21±8.37	0.17±0.03	+15.3±0.6	55.68±2.31	42.89±4.37
1	124.54±7.61	0.17±0.04	+14.8±0.5	56.42±3.39	41.94±4.95
7	134.12±10.82	0.25±0.06	+14.3±0.8	53.45±4.67	40.73±6.37

Abbreviations: PDI, polydispersity index; EE, entrapment efficiency; SD, standard deviation.

mice immunized with Lip E7/CpG and Free E7/CpG showed significantly increased percentages of Tregs (Figure 4A), while there were significant reductions in the percentages of MDSCs and macrophages, compared with control group (Figure 4B and C). Representative dot plots from one mouse (out of three) are presented in Figure 4D–F. In the TME, there were no significant changes in Tregs (Figure 6A), while the reduction in MDSCs and macrophages were the same as those observed in the spleen (Figure 6B and C); representative dot plots from one mouse (out of three) are presented in Figure 6D–F.

Lip E7/CpG Enhanced in vivo CTL Responses

An assay for antigen-specific CTL responses provided additional information on the function of the vaccine formulation. Mice treated with empty liposome did not exhibit any noticeable E7-specific CTL responses. In contrast, those immunized with Free E7/CpG and Lip E7/CpG efficiently eliminated approximately 55% and 60% of E7-pulsed target cells, respectively (Figure 7). These data

suggest that both Free E7/CpG and Lip E7/CpG vaccine elicited potent E7-specific CTL responses in vivo.

Lip E7/CpG Altered the Profiles of Cytokines and Chemokines in the TME

Cytokines and chemokines comprise a complex network of regulating immune cell function and trafficking. To further understand the mechanisms underlying the promotion of immune responses mediated by Lip E7/CpG, we investigated cytokine and chemokine expression profiles in the TME, following treatment. The mRNA levels of IL-12, INF- γ , TNF- α , and IL-2 were significantly increased, while those of IL-4 and TGF- β were significantly decreased. Increases in chemokine mRNA levels, including CCL-3, CXCL-9 and CXCL-10 were also detected (Figure 8).

Lip E7/CpG Significantly Inhibited Tumor Angiogenesis and Proliferation in the TME

Tumor angiogenesis and tumor cell proliferation in response to Lip E7/CpG therapy were also examined.

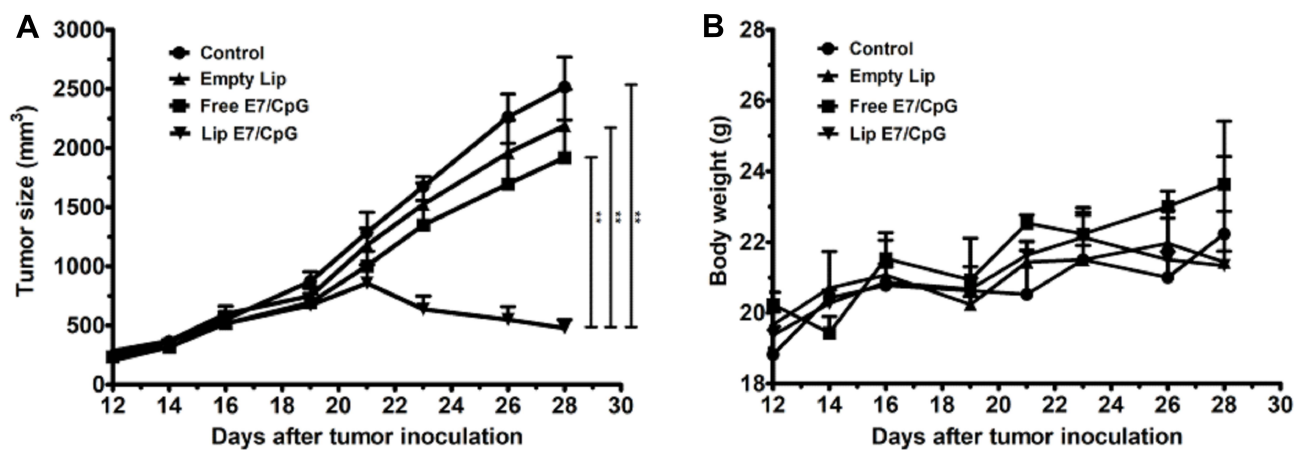


Figure 2 Antitumor activity of vaccine formulation and body weight observed in TC-1 engrafted tumors-bearing mice. *C57BL/6* mice were inoculated with 5×10^5 TC-1 cells on day 0 (n=6). Vaccination was performed on day 12. Tumor growth (A) and body weight (B) were measured every 2–3 days for 16 days. Mice were sacrificed on day 28 and tumors were harvested for further study. Data are presented as mean ± SD. Statistical analyses are indicated (**p < 0.01). Results are from a single experiment in which all targets were tested and they are representative of two to three experiments per tested target.

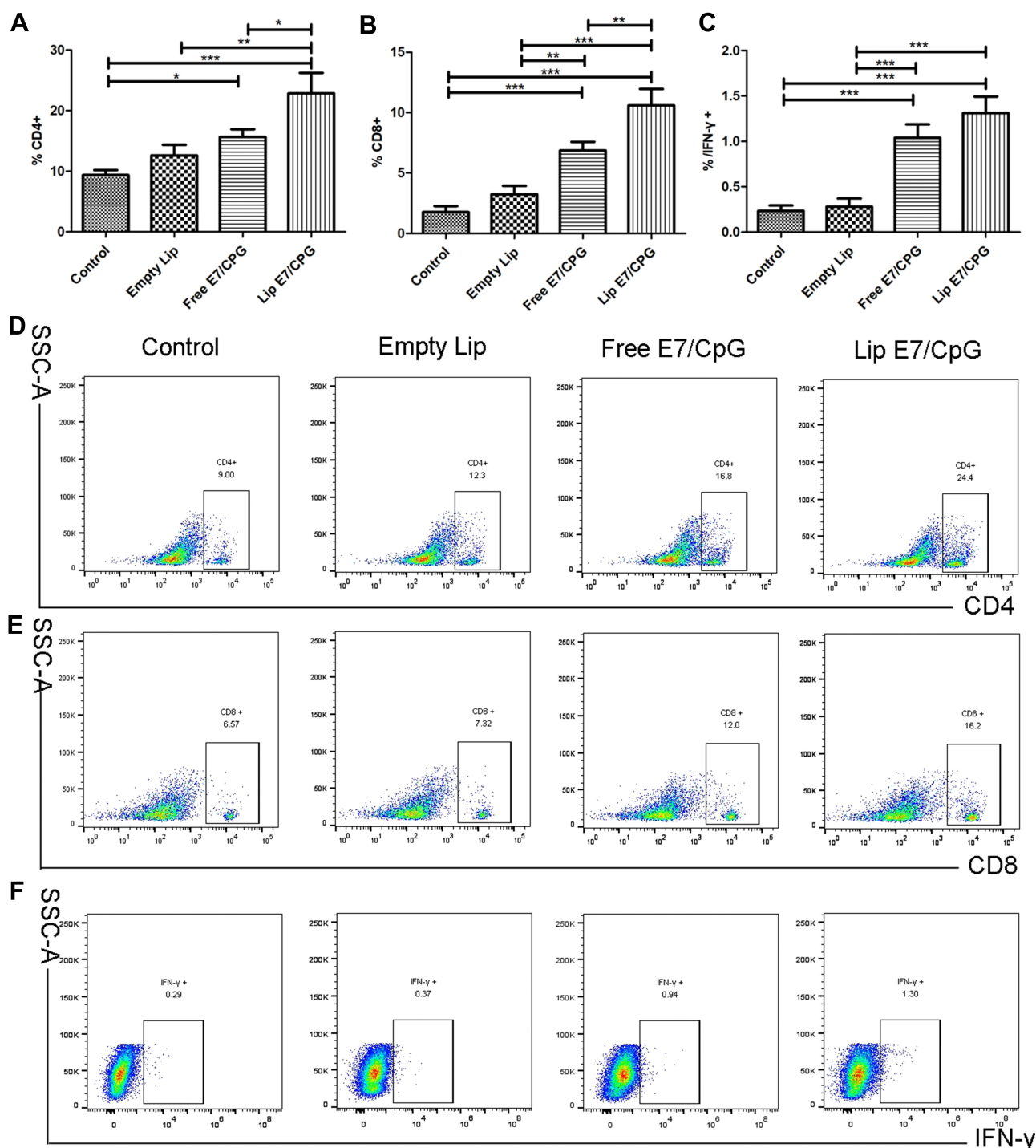


Figure 3 Immune responses induced by the vaccine in spleen. Immunized mice (n=3) were sacrificed on day 28. The frequency of CD4+ cells (A), CD8+ cells (B) and IFN- γ producing cells (C) are shown. Representative dot plots from one mouse (out of three mice) for CD4+ cells (D), and CD8+ cells (E) and IFN- γ producing cells (F) are shown respectively. Data are presented as mean \pm SD. Statistically significant differences are indicated as follow: *P < 0.05, **P < 0.01, ***P < 0.001.

Immunohistochemical staining for CD31 (a vascular endothelial marker), Ki67 (a proliferation marker), and mutant p53 showed that angiogenesis was significantly reduced, while levels of Ki67 and mutant p53 were significantly lower in tumor tissues from mice treated with Lip E7/CpG (Figure 9).

Safety Evaluation of the Lip E7/CpG

No decrease in body weight was observed in any of the groups, indicating no apparent toxicity associated with the treatments (Figure 2B). All mice were dissected and tissue specimens, including heart, liver, spleen, lung and kidney

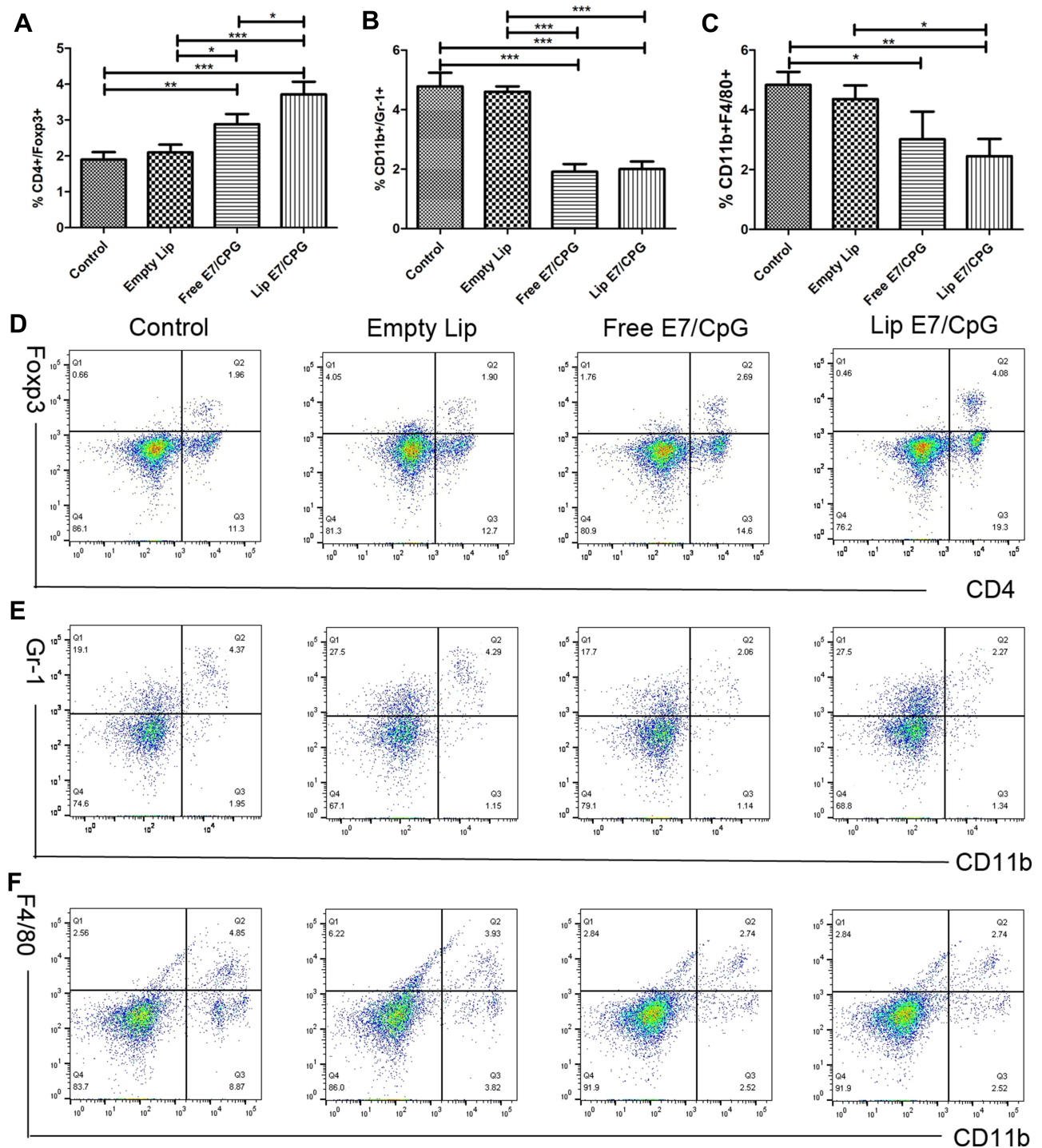


Figure 4 Alteration of systemic immunosuppressive cells induced by the vaccine. Immunized mice (n=3) were sacrificed on day 28. The frequency of Tregs (CD4⁺FoxP3⁺) (A), MDSCs (CD11b⁺Gr-1⁺) (B) and macrophages (CD11b⁺F4/80⁺) (C) are shown. Representative dot plots from one mouse (out of three) for CD4⁺FoxP3⁺ cells (D), CD11b⁺Gr-1⁺ cells (E), and CD11b⁺F4/80⁺ cells (F). Data are presented as mean \pm SD. Statistically significant differences are indicated as follow: *P < 0.05, **P < 0.01, ***P < 0.001.

were harvested. HE staining showed no significant changes in morphology of any major organs in the Lip E7/CpG group (Figure 10).

Discussion

Our previous studies demonstrated that HPV16 E7 43–77 peptide combined with CpG ODN can induce

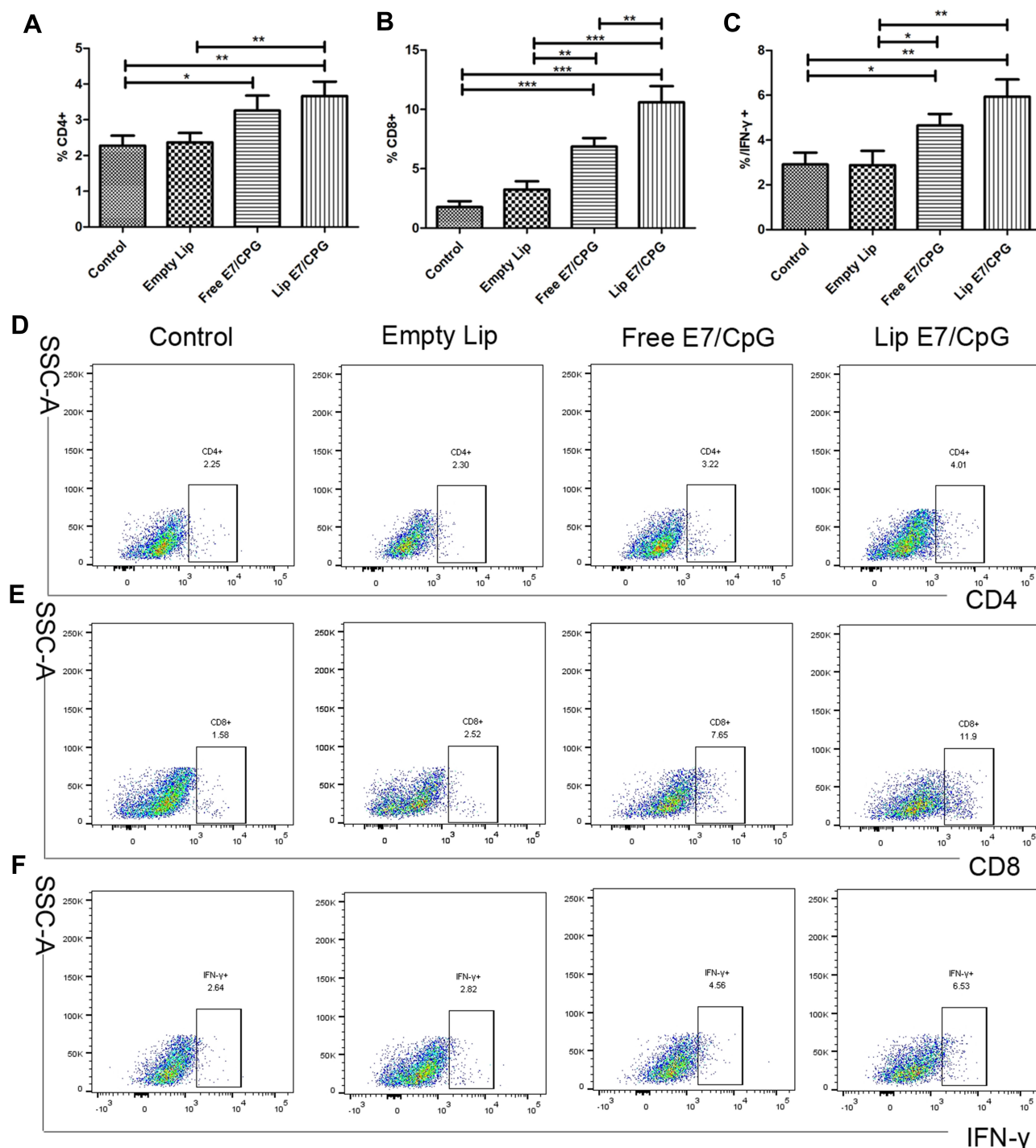


Figure 5 Immune responses induced by the vaccine in the tumors. Immunized mice (n = 3) were sacrificed on day 28. The frequency of CD4+ cells (A), CD8+ cells (B), and IFN-γ-producing cells (C) are presented. Representative dot plots from one mouse (out of three) for CD4+ cells (D), and CD8+ cells (E), and IFN-γ-producing cells (F) are shown. Data are presented as mean ± SD. Statistically significant differences are indicated as follow: *P < 0.05, **P < 0.01, ***P < 0.001.

IFN-γ-producing CD8+ and CD4+ T cells, which contribute to the eradication of small TC-1 grafted tumors in mice.⁷ Nevertheless, several challenges remain to use this treatment approach for large tumors. These challenges could be a reflection of poor platforms that fail to

elicit optimal DC phagocytosis, antigen processing, or presentation by DCs, or of suboptimal adjuvants. Furthermore, free peptides are likely to be rapidly cleared before they reach the DCs. There may also be a risk of inducing specific tolerance after systemic

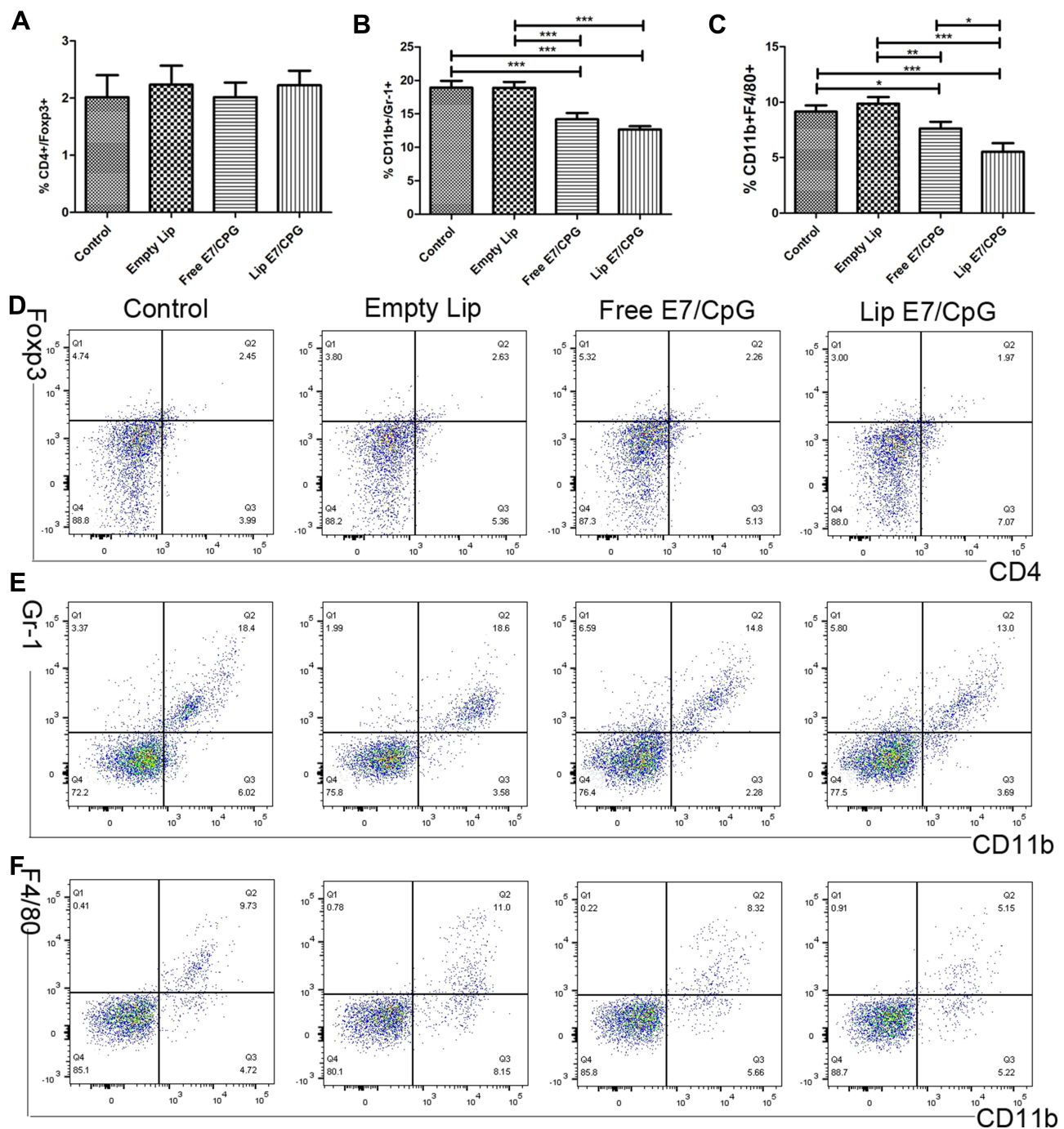


Figure 6 Alterations in immunosuppressive cell levels induced by the vaccine in the tumors. Immunized mice ($n = 3$) were sacrificed on day 28. The frequency of Tregs (CD4+Foxp3+) (A), MDSCs (CD11b+Gr-1+) (B), and macrophages (CD11b+F4/80+) (C) are shown. Representative dot plots from one mouse (out of three) for CD4+Foxp3+ cells (D), CD11b+Gr-1+ cells (E), and CD11b+F4/80+ cells (F) are shown. Data are presented as mean \pm SD. Statistically significant differences are indicated as follow: * $P < 0.05$, ** $P < 0.01$, *** $P < 0.001$.

delivery of high doses of peptides, particularly in the absence of an appropriate DC activator. Hence, efficient DC-targeting is needed to overcome these drawbacks.

Mannose-modified vectors can specifically target and activate DC-mediated antitumor activities through mannose receptors.^{20,24,25} Cationic liposomes have shown

great potential as effective vaccine delivery systems.^{26–28}

Based on the rationale that mannose synergistically with lipid as previously reported,²² we developed a vaccination strategy by assembling DC-targeting mannose on the surface of cationic liposomes which were loaded with HPV16 E7 peptide and CpG ODN. Our results

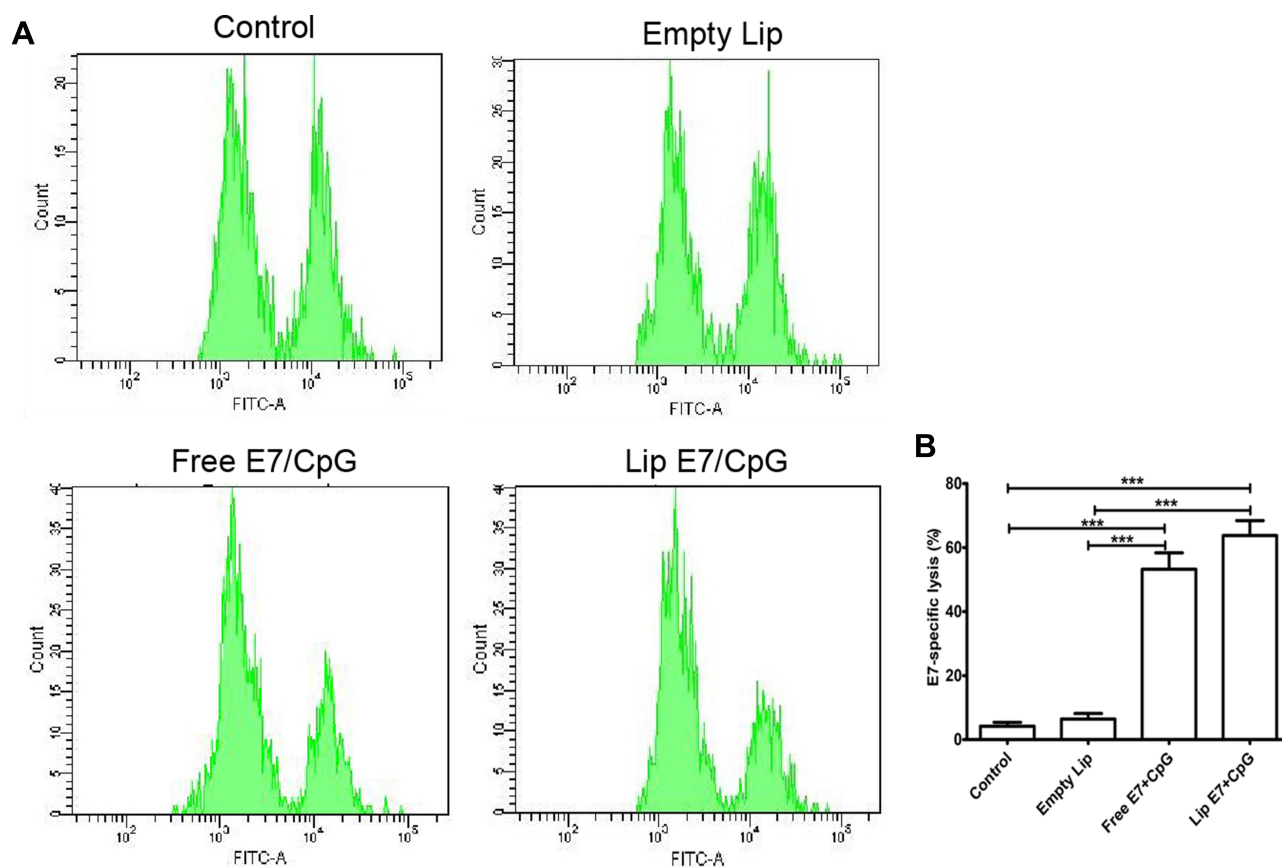


Figure 7 In vivo CTL responses following vaccination. *C57BL/6* mice were subcutaneously injected with free and liposome containing E7 peptide and CpG ODN on day 0; splenocytes from naïve mice were pulsed with Ova or E7 peptide and stained with low (Ova) or high (E7) concentrations of CFSE, respectively. Cells were then mixed and injected into the vaccinated mice ($n = 3$). After 18 h, splenocytes from the vaccinated mice were analyzed by flow cytometry and the degree of lysis calculated according to a published equation. E7-specific lysis (A) and representative graphs for each group (B). Statistically significant differences are indicated as follow: *** $P < 0.001$.

demonstrate that this Lip E7/CpG vaccine can significantly inhibit growth of large TC-1 grafted tumors in a mouse model.

The effector mechanism of tumor vaccines is to elicit tumor antigen-specific cellular and humoral immune responses, and a balance between these is essential to achieve and maintain immune homeostasis.²⁹ Cellular immunity is important for clearing tumor cells, with CTLs specifically regarded as major anti-tumor effectors. CD4⁺ T cells assist in priming the generation, expansion and maintenance of CTLs, as well as in orchestrating antibody production. Moreover, there is evidence that CD4⁺ T cells contribute to anti-tumor immunity.^{30,31} DCs take up and process antigens and present the antigen peptide to CD8⁺ T cells in the context of an MHC I-peptide complex. Further, they also present antigen peptide complexes to CD4⁺ T cells (Helper T cells, Th) via the classical antigen presentation pathway, in the form of MHC II-peptide complexes.^{32,33}

Therapeutic studies showed that Lip E7/CpG can inhibit tumor growth (Figure 2), and we also investigated

whether it enhances intake processing and presentation of antigens to activate CD4⁺ and CD8⁺ T cells. Lip E7/CpG effectively increased the number of CD4⁺ T cells, CD8⁺ T cells and IFN- γ -producing cells, thus inducing an effective cellular immune response. Meanwhile, it significantly reduced the number of MDSCs and macrophages. Further, numbers of inhibitory Tregs were increased in the vaccine group, consistent with previous reports.^{34,35} Collectively, our results indicate that this liposomal vaccine has potential for use in treatment of advanced cervical cancer in the clinic.

Additionally, to further explore the mechanisms underlying the reversion of the immunosuppressive TME mediated by Lip E7/CpG, we investigated cytokine and chemokine expression profiles in the TME in response to treatment. Cytokines are important protein mediators of immune responses, and the cytokine content of the TME can influence the balance of immunosuppressive and immunosupportive factors.³⁶ IL-12 is a potent inducer of Th1 responses, and we detected increased levels of IL-12

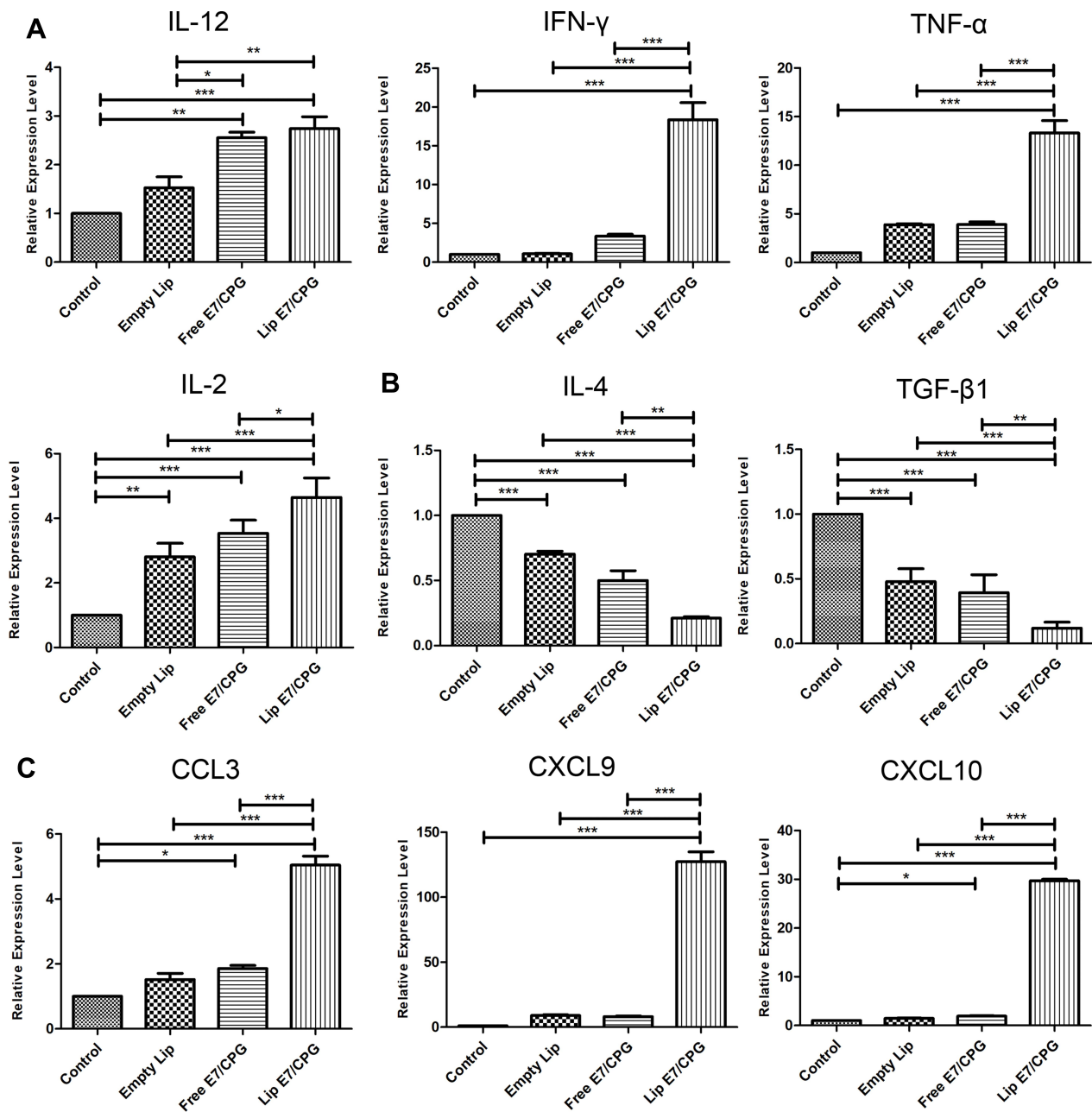


Figure 8 Local tumoral cytokine and chemokine levels after vaccination. *C57BL/6* mice were inoculated with 5×10^5 TC-1 cells on day 0. The vaccine was given on day 12. Mice were sacrificed on day 28, and tumors were collected for Th1 type cytokine (**A**), Th2 type cytokine (**B**), and chemokine (**C**) detection using RT-PCR. Results are displayed as mean \pm SD. Statistically significant differences are indicated as follows: * $P < 0.05$, ** $P < 0.01$, *** $P < 0.001$.

as well as IL-2, INF- γ and TNF- α , in the Lip E7/CpG group (Figure 8) demonstrating the potential of Lip E7/CpG to induce polarization of the immune response toward a Th1 immune response, which is more effective in eliciting anti-tumor immunity. TGF- β is associated with the induction of immunosuppression by MDSCs, Tregs and M2-tumor-associated macrophages.^{37–39} Decreased TGF- β in response to Lip E7/CpG may result from a decreased number in the cells that produce this factor,

leading to a reduced inhibitory effect on a variety of immune cells. Moreover, CCL3 plays a critical role in recruiting cells with distinct immune phenotypes to intra-tumoral sites and regulating lymph node homing of DC subsets.⁴⁰ Overexpression of CXCL-9 and CXCL-10 has been a major focus of research, since it regulates differentiation of naïve T cells to a T helper 1 (Th1) phenotype, and regulates migration of immune cells to their focal sites.⁴¹ Higher levels of CCL3, CXCL-9, and CXCL-10

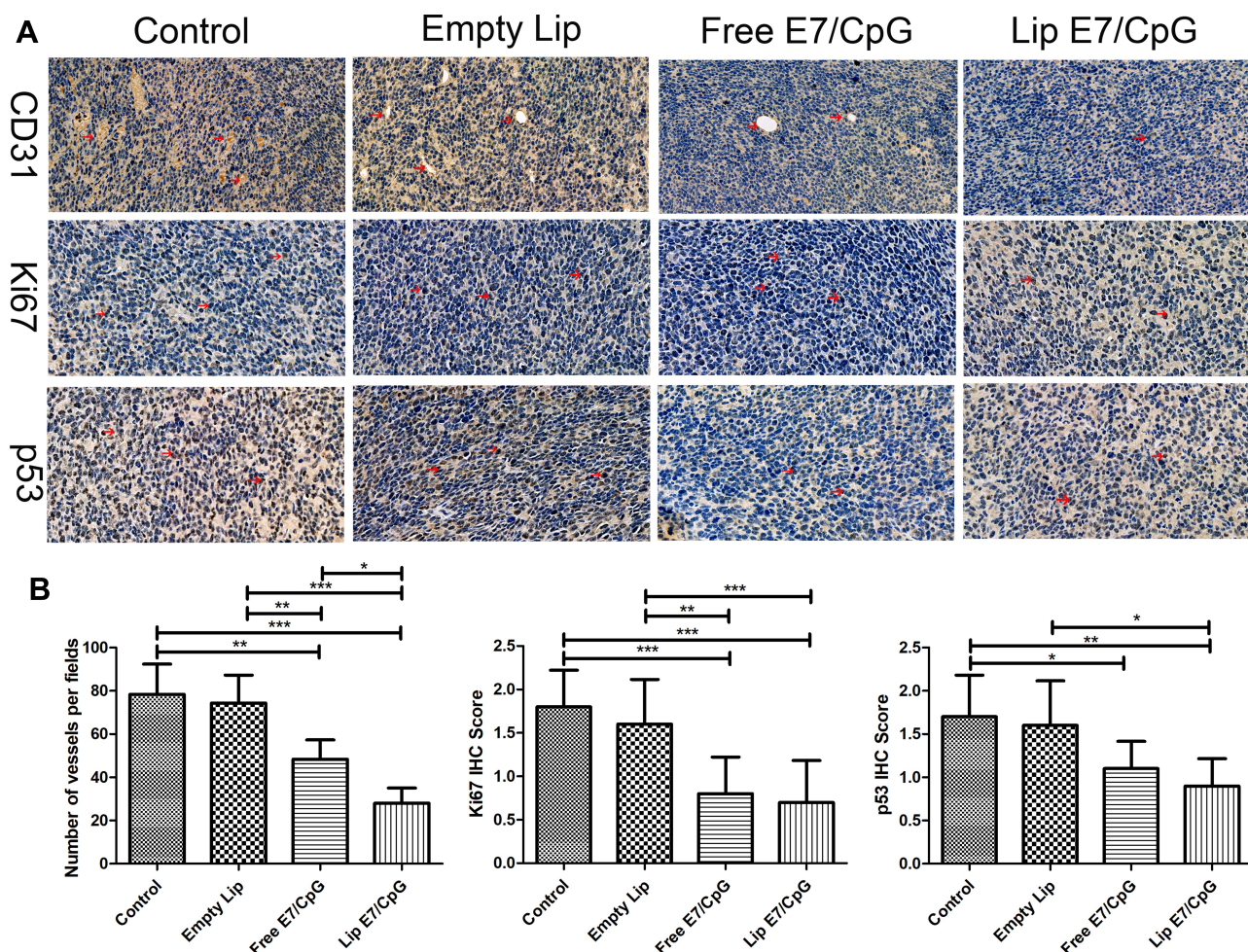


Figure 9 Effects of the Lip E7/CpG on angiogenesis, cell proliferation and malignancy identified by immunohistochemical staining of tumor tissue sections from mice using anti-CD31 antibody (400×), anti-Ki67 antibody (400×), and anti-p53 antibody (400×) (A). Red arrows indicate positive cells. Quantitative analysis (B). Data are presented as the means ± SD for each group of tumors. Statistically significant differences are indicated as follow: *P < 0.05, **P < 0.01, ***P < 0.001.

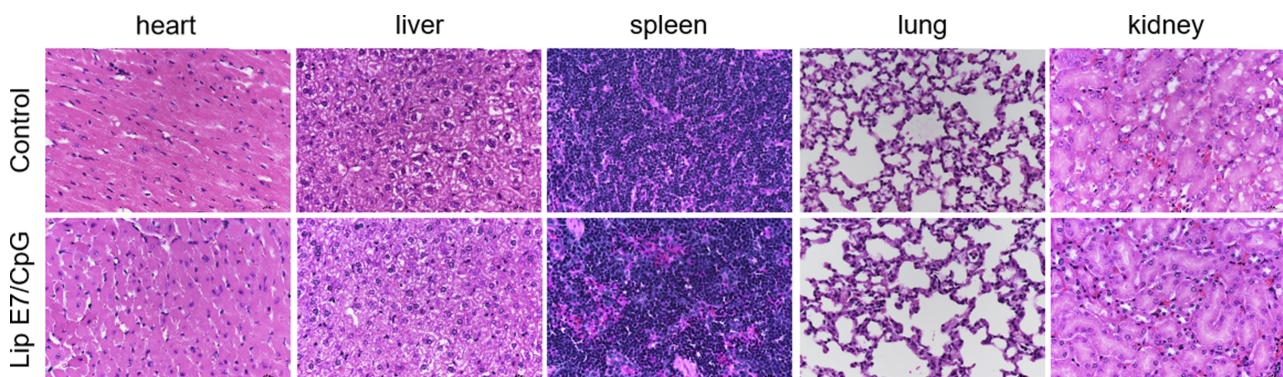


Figure 10 The toxicity of the vaccine was evaluated in organs from vaccinated mice by HE staining. *C57BL/6* mice were inoculated with 5×10^5 TC-1 cells on day 0. The vaccine was administered on day 12. Mice were sacrificed on day 28, and major organs were collected. Representative histologic sections illustrating the health of the heart, liver, spleen, lung, and kidney. Lip E7/CPG was well tolerated and did not result in any significant damage to the major organs of the mice.

in response to Lip E7/CpG (Figure 8) favor an anti-tumor immune response in the TME. Such immune modulation, although insufficient to inhibit tumor growth alone, will greatly facilitate the activity of Lip E7/CpG.

We also examined tumor angiogenesis, tumor cell proliferation, and p53 in response to Lip E7/CpG therapy. Lip E7/CpG significantly reduced vessel concentration, consistent with a previous report showing that immunotherapies can

reduce tumor vasculature through release of IFN I and II in the TME.⁹ Staining for the proliferation marker, Ki67, and p53 were significantly reduced in the Lip E7/CpG treatment group, consistent with the previously reported therapeutic HPV vaccine research.^{42,43}

This study demonstrated that Lip E7/CpG can efficiently enhance anti-tumor effects in mice grafted with large TC-1 tumors. Nonetheless, the relatively short follow-up of tumor growth after vaccination is a limitation of this study. In future research, we will prolong the follow-up period and investigate the long-term protective effects, as well as the immune memory, induced by the vaccination. Moreover, we will establish an orthotopic vaginal/cervix tumor model, as a surrogate for cervical cancer, to further evaluate the tumor inhibition effects of the Lip E7/CpG vaccine in vivo.

Conclusion

In summary, Lip E7/CpG efficiently enhanced anti-large TC-1 grafted tumor effects in mice by improving cellular immune responses and alleviating immune suppression. Although the treatment efficacy of the liposomal vaccine was somewhat limited, it significantly inhibited tumor cell proliferation, thus reducing tumor growth, which suggests mannose-modified liposomes are a promising vaccine delivery strategy for cancer immunotherapy.

Abbreviations

HPV, human papillomavirus; CpG ODN, CpG oligodeoxynucleotides; MDSC, myeloid-derived suppressor cells; TME, tumor microenvironment; APCs, antigen presenting cells; DCs, dendritic cells; Tregs, regulatory T cells; MHC-I, histocompatibility complex class I; MHC-II, histocompatibility complex class II; CTL, cytotoxic T lymphocyte; TLR9, Toll-like receptor 9; SPC, L-alpha-phosphatidyl choline; CHOL, cholesterol; DSPE-PEG-2000, 1,2-distearoyl-*sn*-glycero-3-phosphoethanolamine-N-[methoxy (polyethylene glycol-2000)]; DSPE-PEG-NHS, 1,2-distearoyl-*sn*-glycero-3-phosphoethanolamine-N-[succinimidyl (polyethylene glycol)-2000]; DOTAP, 1,2-dioleoyl-3-trimethylammonium-propane chloride salt; HE, hematoxylin and eosin; ANOVA, analysis of variance; EE, encapsulation efficiency; Th1, T helper 1.

Acknowledgments

This work was supported by the National Natural Science Foundation of China (No. 81472439, 81803461), the Liaoning Provincial Natural Science Foundation of China

(No.20180550760) and the Scientific Research Fund of Liaoning Provincial Education Department (No. L2010709).

Disclosure

The authors report no conflicts of interest in this work.

References

- Denny L. Cervical cancer: prevention and treatment. *Discov Med*. 2012;14(75):125–131.
- Mavundza EJ, Wiyeh AB, Mahasha PW, Halle-Ekane G, Wiysonge CS. A systematic review of immunogenicity, clinical efficacy and safety of human papillomavirus vaccines in people living with the human immunodeficiency virus. *Hum Vaccin Immunother*. 2020;16:426–435.
- Murillo R, Ordóñez-Reyes C. Human papillomavirus (HPV) vaccination: from clinical studies to immunization programs. *Int J Gynecol Cancer*. 2019;29(8):1317–1326. doi:10.1136/ijgc-2019-000582
- Stevanovic S, Draper LM, Langhan MM, et al. Complete regression of metastatic cervical cancer after treatment with human papillomavirus-targeted tumor-infiltrating T cells. *J Clin Oncol*. 2015;33(14):1543–1550. doi:10.1200/JCO.2014.58.9093
- Cerezo D, Pena MJ, Mijares M, Martínez G, Blanca I, De Sanctis JB. Peptide vaccines for cancer therapy. *Recent Pat Inflamm Allergy Drug Discov*. 2015;9(1):38–45.
- Parmiani G, Russo V, Maccalli C, Parolini D, Rizzo N, Maio M. Peptide-based vaccines for cancer therapy. *Hum Vaccin Immunother*. 2014;10(11):3175–3178. doi:10.4161/hv.29418
- Yang Y, Che Y, Zhao Y, Wang X. Prevention and treatment of cervical cancer by a single administration of human papillomavirus peptide vaccine with CpG oligodeoxynucleotides as an adjuvant in vivo. *Int Immunopharmacol*. 2019;69:279–288. doi:10.1016/j.intimp.2019.01.024
- Liotta LA, Kohn EC. The microenvironment of the tumour-host interface. *Nature*. 2001;411(6835):375–379. doi:10.1038/35077241
- Devaud C, John LB, Westwood JA, Darcy PK, Kershaw MH. Immune modulation of the tumor microenvironment for enhancing cancer immunotherapy. *Oncoimmunology*. 2013;2(8):e25961. doi:10.4161/onci.25961
- Mellman I, Steinman RM. Dendritic cells: specialized and regulated antigen processing machines. *Cell*. 2001;106(3):255–258. doi:10.1016/S0092-8674(01)00449-4
- Steinman RM. Decisions about dendritic cells: past, present, and future. *Annu Rev Immunol*. 2012;30:1–22. doi:10.1146/annurev-immunol-100311-102839
- Tacke PJ, de Vries IJM, Torensma R, Figdor CG. Dendritic-cell immunotherapy: from ex vivo loading to in vivo targeting. *Nat Rev Immunol*. 2007;7(10):790–802. doi:10.1038/nri2173
- Geijtenbeek TBH, Torensma R, van Vliet SJ, et al. Identification of DC-SIGN, a novel dendritic cell-specific ICAM-3 receptor that supports primary immune responses. *Cell*. 2000;100(5):575–585. doi:10.1016/S0092-8674(00)80693-5
- Bonifaz LC, Bonnyay DP, Charalambous A, et al. In vivo targeting of antigens to maturing dendritic cells via the DEC-205 receptor improves T cell vaccination. *J Exp Med*. 2004;199(6):815–824. doi:10.1084/jem.20032220
- van Broekhoven CL, Parish CR, Demangel C, Britton WJ, Altin JG. Targeting dendritic cells with antigen-containing liposomes: a highly effective procedure for induction of antitumor immunity and for tumor immunotherapy. *Cancer Res*. 2004;64(12):4357–4365.
- Miconnet I, Koenig S, Speiser D, et al. CpG are efficient adjuvants for specific CTL induction against tumor antigen-derived peptide. *J Immunol*. 2002;168(3):1212–1218. doi:10.4049/jimmunol.168.3.1212

17. Faisal SM, Yan W, McDonough SP, Chang YF. Leptospira immunoglobulin-like protein A variable region (LigAvar) incorporated in liposomes and PLGA microspheres produces a robust immune response correlating to protective immunity. *Vaccine*. 2009;27(3):378–387. doi:10.1016/j.vaccine.2008.10.089
18. Lin YY, Kao HW, Li JJ, et al. Tumor burden talks in cancer treatment with PEGylated liposomal drugs. *PLoS One*. 2013;8(5):e63078. doi:10.1371/journal.pone.0063078
19. He LZ, Crocker A, Lee J, et al. Antigenic targeting of the human mannose receptor induces tumor immunity. *J Immunol*. 2007;178(10):6259–6267. doi:10.4049/jimmunol.178.10.6259
20. Keler T, Ramakrishna V, Fanger MW. Mannose receptor-targeted vaccines. *Expert Opin Biol Ther*. 2004;4(12):1953–1962. doi:10.1517/14712598.4.12.1953
21. Che Y, Yang Y, Suo J, An Y, Wang X. Induction of systemic immune responses and reversion of immunosuppression in the tumor microenvironment by a therapeutic vaccine for cervical cancer. *Cancer Immunol Immunother*. 2020. doi:10.1007/s00262-020-02651-3
22. Zhao Y, Huo M, Xu Z, Wang Y, Huang L. Nanoparticle delivery of CDDO-Me remodels the tumor microenvironment and enhances vaccine therapy for melanoma. *Biomaterials*. 2015;68:54–66. doi:10.1016/j.biomaterials.2015.07.053
23. Zhao Y, Hu HY, Sun DR, et al. Dynamic alterations in the CaV1.2/CaM/CaMKII signaling pathway in the left ventricular myocardium of ischemic rat hearts. *DNA Cell Biol*. 2014;33(5):282–290. doi:10.1089/dna.2013.2231
24. Wang F, Xiao W, Elbahnasawy MA, et al. Optimization of the linker length of mannose-cholesterol conjugates for enhanced mRNA delivery to dendritic cells by liposomes. *Front Pharmacol*. 2018;9:980. doi:10.3389/fphar.2018.00980
25. Xu Z, Ramishetti S, Tseng YC, Guo S, Wang Y, Huang L. Multifunctional nanoparticles co-delivering Trp2 peptide and CpG adjuvant induce potent cytotoxic T-lymphocyte response against melanoma and its lung metastasis. *J Control Release*. 2013;172(1):259–265. doi:10.1016/j.jconrel.2013.08.021
26. Christensen D, Korsholm KS, Andersen P, Agger EM. Cationic liposomes as vaccine adjuvants. *Expert Rev Vaccines*. 2011;10(4):513–521.
27. Sahdev P, Ochyl LJ, Moon JJ. Biomaterials for nanoparticle vaccine delivery systems. *Pharm Res-Dordr*. 2014;31(10):2563–2582. doi:10.1007/s11095-014-1419-y
28. Khademi F, Taheri RA, Momtazi-Borojeni AA, Farnoosh G, Johnston TP, Sahebkar A. Potential of cationic liposomes as adjuvants/delivery systems for tuberculosis subunit vaccines. *Rev Physiol Bioch P*. 2018;175:47–69.
29. Becker T, Loch G, Beyer M, et al. FOXO-dependent regulation of innate immune homeostasis. *Nature*. 2010;463(7279):369–373. doi:10.1038/nature08698
30. Mahnke K, Guo M, Lee S, et al. The dendritic cell receptor for endocytosis, DEC-205, can recycle and enhance antigen presentation via major histocompatibility complex class II-positive lysosomal compartments. *J Cell Biol*. 2000;151(3):673–683. doi:10.1083/jcb.151.3.673
31. Albert ML, Pearce SF, Francisco LM, et al. Immature dendritic cells phagocytose apoptotic cells via $\alpha\text{v}\beta 5$ and CD36, and cross-present antigens to cytotoxic T lymphocytes. *J Exp Med*. 1998;188(7):1359–1368. doi:10.1084/jem.188.7.1359
32. Joffre OP, Segura E, Savina A, Amigorena S. Cross-presentation by dendritic cells. *Nat Rev Immunol*. 2012;12(8):557–569. doi:10.1038/nri3254
33. Kikete S, Chu X, Wang L, Bian Y. Endogenous and tumour-derived microRNAs regulate cross-presentation in dendritic cells and consequently cytotoxic T cell function. *Cytotechnology*. 2016;68(6):2223–2233. doi:10.1007/s10616-016-9975-0
34. Karkada M, Quinton T, Blackman R, Mansour M. Tumor inhibition by depovax-based cancer vaccine is accompanied by reduced regulatory/suppressor cell proliferation and tumor infiltration. *ISRN Oncol*. 2013;2013:753427. doi:10.1155/2013/753427
35. Weir GM, Hrytsenko O, Stanford MM, et al. Metronomic cyclophosphamide enhances HPV16E7 peptide vaccine induced antigen-specific and cytotoxic T-cell mediated antitumor immune response. *Oncimmunology*. 2014;3(8):e953407. doi:10.4161/21624011.2014.953407
36. Shurin MR, Lu L, Kalinski P, Stewart-Akers AM, Lotze MT. Th1/Th2 balance in cancer, transplantation and pregnancy. *Springer Semin Immunopathol*. 1999;21(3):339–359. doi:10.1007/BF00812261
37. Marvel D, Gabrilovich DI. Myeloid-derived suppressor cells in the tumor microenvironment: expect the unexpected. *J Clin Invest*. 2015;125(9):3356–3364. doi:10.1172/JCI80005
38. Schmidt A, Oberle N, Krammer PH. Molecular mechanisms of treg-mediated T cell suppression. *Front Immunol*. 2012;3:51. doi:10.3389/fimmu.2012.00051
39. Sawa-Wejksza K, Kandefer-Szerszen M. Tumor-associated macrophages as target for antitumor therapy. *Arch Immunol Ther Ex*. 2018;66(2):97–111. doi:10.1007/s00005-017-0480-8
40. Schaller TH, Batich KA, Suryadevara CM, Desai R, Sampson JH. Chemokines as adjuvants for immunotherapy: implications for immune activation with CCL3. *Expert Rev Clin Immunol*. 2017;13(11):1049–1060. doi:10.1080/17446666X.2017.1384313
41. Tannenbaum CS, Tubbs R, Armstrong D, Finke JH, Bukowski RM, Hamilton TA. The CXC chemokines IP-10 and Mig are necessary for IL-12-mediated regression of the mouse RENCA tumor. *J Immunol*. 1998;161(2):927–932.
42. Hancock G, Hellner K, Dorrell L. Therapeutic HPV vaccines. *Best Pract Res Clin Obstet Gynaecol*. 2018;47:59–72. doi:10.1016/j.bpobgyn.2017.09.008
43. Shiohara S, Shiozawa T, Miyamoto T, et al. Expression of cyclins, p53, and Ki-67 in cervical squamous cell carcinomas: overexpression of cyclin A is a poor prognostic factor in stage Ib and II disease. *Virchows Arch*. 2005;446(6):626–633. doi:10.1007/s00428-005-1252-0

International Journal of Nanomedicine

Publish your work in this journal

The International Journal of Nanomedicine is an international, peer-reviewed journal focusing on the application of nanotechnology in diagnostics, therapeutics, and drug delivery systems throughout the biomedical field. This journal is indexed on PubMed Central, MedLine, CAS, SciSearch®, Current Contents®/Clinical Medicine,

Journal Citation Reports/Science Edition, EMBase, Scopus and the Elsevier Bibliographic databases. The manuscript management system is completely online and includes a very quick and fair peer-review system, which is all easy to use. Visit <http://www.dovepress.com/testimonials.php> to read real quotes from published authors.

Submit your manuscript here: <https://www.dovepress.com/international-journal-of-nanomedicine-journal>